Collisionless reconnection using Alfvén wave radiation resistance

P. M. Bellan
Caltech, Pasadena, California 91125

(Received 24 November 1997; accepted 8 June 1998)

Patchy magnetic reconnection involves transient field-aligned current filaments. The spatial localization, transient time-dependence, and orientation of these current filaments means they must radiate torsional Alfvén waves. Radiation of wave energy does not come for free—it must load the current which acts as the radiative source. This loading (radiation resistance) is proposed as the energy sink required for collisionless magnetic reconnection to proceed. Radiation resistance for both inertial and kinetic Alfvén waves is calculated and, for highly collisionless plasmas, is shown to exceed by a substantial factor both Spitzer resistivity and the effective resistance due to the direct acceleration of electrons (inertial loading). The radiation resistivity is shown to provide the magnetic field diffusivity required for magnetic fields to diffuse across the assumed width of the current filament on the time scale of the reconnection. It is also shown that Landau damping of the radiated waves results in the generation of energetic, field-aligned particles: in the $\beta \ll m_e/m_i$ regime the energetic particles are electrons while in the $m_e/m_i \ll \beta \ll 1$ regime, the energetic particles are ions.
 [S1070-664X(98)02909-7]

I. INTRODUCTION

Magnetic reconnection allows the global magnetic topology of a magnetized plasma to relax to a lower energy state; i.e., magnetic reconnection involves *removing* energy from the system.

The topology of reconnection is sketched in Fig. 1 and, in particular, the ''after'' sketch in Fig. 1(c) shows the x-point geometry that is the hallmark of reconnection. Ideal magnetohydrodynamics (MHD) cannot describe reconnection because ideal MHD does not permit the plasma-frame electric fields required to evolve an x-point and absorb energy from the system. Resistive MHD does allow plasma-frame electric fields and provides a compelling, self-consistent description of magnetic reconnection based on the diffusion of magnetic field lines across a very narrow layer. The diffusion coefficient for this resistive reconnection is $D_{res}=\eta_{Spitz}/\mu_0$ where η_{Spitz} is the conventional Spitzer resistivity,

$$\eta_{Spitz}=\frac{m_e}{\tau_{ei}ne^2}=\frac{c^2\mu_0}{\tau_{ei}\omega_{pe}^2}, \tag{1}$$

and τ_{ei} is the electron–ion collision time. For many important situations τ_{ei} is much too large for the Spitzer resistivity to explain observed reconnection rates. There is consequently great interest in finding collisionless mechanisms which would allow the magnetic topology to relax to a lower energy state. The main such mechanisms considered to date are electron inertia (finite m_e) and Hall dynamics (finite ω/ω_{ci}).

Hall dynamics allows magnetic field line motion in the center of mass frame, but not in the electron frame. This motion cannot change the topology because no dissipation is introduced. Hall dynamics may therefore catalyze collisionless reconnection, but cannot provide a complete description. In contrast, electron inertia provides a possible energy sink because work must be performed to accelerate the electrons[1–4] carrying the transient currents associated with reconnection. The power required to accelerate these electrons is $P_{inertia}\simeq nm_e v_e^2/2\tau_{acc}$ where τ_{acc} is the characteristic acceleration time. Since $J=-nev_z$ the effective resistivity associated with electron inertia is

$$\eta_{inertia}=P/J^2=\frac{c^2\mu_0}{2\tau_{acc}\omega_{pe}^2}. \tag{2}$$

The associated magnetic diffusion coefficient is $D_{inertia}=\eta_{inertia}/\mu_0=c^2/2\omega_{pe}^2\tau_{acc}$ so that the diffusion width associated with electron inertia is the electron skin depth c/ω_{pe}. Detailed models of collisionless reconnection show[1,4,5] that the perpendicular scale length for electron-inertia reconnection is indeed $\sim c/\omega_{pe}$. Comparing Eqs. (1) and (2) shows that $\eta_{inertia}/\eta_{Spitz}=\tau_{ei}/2\tau_{acc}$. Thus, if electrons are accelerated to the velocity $v_z=-J/ne$ in a time shorter than the electron–ion collision time, inertial loading will dominate over conventional resistive loading.

The purpose of this paper is to demonstrate that *radiation resistance* resulting from the emission of Alfvén waves produces an effective loading which, in certain situations, can greatly exceed the resistivity given by Eqs. (1) and (2) and should therefore remove energy from the system at a rate much greater than predictions based on Spitzer resistivity or electron inertia. Radiation resistance is inherently nonlocal because it involves the combined effects of time retardation, finite source dimension, and boundaries at infinity. These effects are such that radiation resistance cannot be characterized by simply adding another term to the system of equations. Equivalently, radiation resistance cannot be described[6] by classical circuit theory because classical circuit theory does not take into account time retardation.

The essence of our argument is as follows: (i) magnetic reconnection necessarily involves localized, transient field-

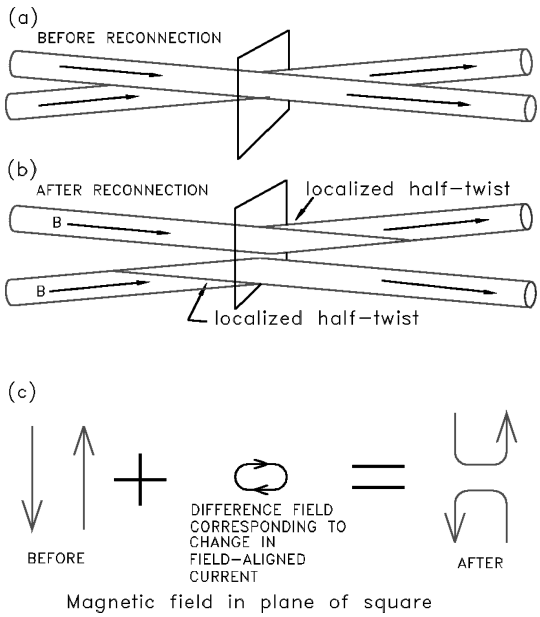

FIG. 1. (a) Two nearly coaxial adjacent flux tubes before reconnection. (b) Flux tubes after localized reconnection. Each flux tube now has a half twist at location of reconnection. (c) The field line projection in the x-y plane at axial location $z=0$. Note that the difference between before and after situations corresponds to a field-aligned current.

aligned currents; (ii) these localized, transient, field-aligned currents must radiate torsional waves; (iii) radiation of these torsional Alfvén waves must consequently resistively load the transient current; (iv) this resistive loading provides the effective dissipation essential for reconnection to occur.

Modeling radiation resistance requires allowing the radiation to escape: the plasma cannot be in a closed conducting box or be characterized by periodic boundary conditions, because standing waves would then develop which would reflect power back to the antenna, exactly balancing the emitted power. Standard reconnection models invariably assume that the z direction is ignorable or the system is periodic in the z direction; either assumption prevents radiation from escaping to infinity and so artificially suppresses radiation resistance. These standard assumptions also imply that magnetic reconnection is uniformly (or periodically) distributed in the z direction. In particular, if the z direction is assumed ignorable [i.e., a two-dimensional (2D) model], then all points along a flux tube are assumed to undergo simultaneous reconnection. On the other hand, if the z direction is assumed periodic with periodicity $2\pi/k_z$, then the dynamics of any given point along a flux tube must be duplicated simultaneously by all points separated by integral multiples of $2\pi/k_z$. Since information propagates at the Alfvén velocity for the time-scales of interest, these assumptions imply a violation of causality because points separated by more than an Alfvén propagation time would have to act synchronously without means of communication.

In reality, magnetic reconnection is not uniform in the z direction, and except for the special case of axisymmetric toroidal systems (e.g., tokamaks, reversed field pinches), magnetic reconnection is also not periodic in the z direction. Instead, magnetic reconnection is typically localized in three dimensions (patchy). All the elements of a localized patch must be in nearly instantaneous communication with each other because, if the elements of a patch are not in good communication with each other, then the patch might just as well be split into independent sub-patches. Unless external means ensure simultaneity along the z direction of a patch, the z-extent of the patchy reconnection region must be smaller than the Alfvén propagation distance corresponding to the characteristic time scale. In other words, if ω is the characteristic frequency of the reconnection process and h is the axial extent of the reconnection region, then in order to have synchronization along the z direction over the axial extent of the reconnection region, it is necessary to have

$$\omega h < v_A . \tag{3}$$

II. TOPOLOGY OF RECONNECTION, MAGNETIC HELICITY, AND TORQUE PROPAGATION

Figure 1 shows that after the localized reconnection of two initially slightly nonparallel straight flux tubes, the reconnected flux tubes must each have a localized half-twist with the same chirality. This is consistent with helicity conservation as discussed by Pfister and Gekelman;[7] the helicity $H=\Phi^2$ due to the crossing of the two flux tubes before reconnection equals the sum of the helicities $H=\Phi^2/2$ of each of the half-twisted flux tubes after reconnection. However, the system cannot remain in the state shown in Fig. 1(b) because the localized twists in Fig. 1(b) are *not* an equilibrium state.[8,9] This is because a localized twist corresponds to an axially localized filament of field-aligned current. In order to satisfy $\nabla\cdot\mathbf{J}=0$ the endpoints of such a current filament must connect to radial inward and outward currents (here radial means relative to the flux tube axis). These radial currents exert a de-twisting torque on the flux tube which annihilates the original twist and creates new twists which propagate in the form of torsional Alfvén waves away from the reconnection region.

Thus, even without invoking specific mathematical models, it is clear that localized reconnection necessarily involves radiation of torsional Alfvén waves away from the reconnection region.

III. LOCALIZED RECONNECTION AND ALFVÉN WAVE RADIATION

Our picture of reconnection thus differs from previous models because we assume (i) the reconnection region is localized to a region of *finite* axial extent h and (ii) the reduction of magnetic energy necessary to change magnetic topology is accomplished by *radiation* of torsional Alfvén waves away from the reconnection region. As support for our hypothesis, we note that experiments[10] in the electron magnetohydrodynamic (EMHD) regime have shown that EMHD reconnection is associated with broadband radiation of whistler waves, a high frequency wave which likely plays a role in EMHD similar to that of the Alfvén waves discussed here. MHD descriptions of torsional Alfvén waves cannot be used to model radiation resistance, because radiation resistance requires finite E_z. Thus, non-MHD torsional Alfvén waves

with finite E_z must be considered. The nature of non-MHD torsional Alfvén waves depends strongly on the plasma β_e (where $\beta_e \equiv 2\mu_0 n\kappa T_e/B^2$). This β_e dependence corresponds to a dependence on the ratio of the Alfvén velocity v_A to the electron thermal velocity v_{Te}.

IV. TAXONOMY OF NON-MHD SHEAR ALFVÉN WAVES

A. Inertial Alfvén waves

If $v_A > v_{Te}$ (which corresponds to $\beta_e < m_e/m_i$) then electron inertia effects govern the wave dynamics. For slab geometry with $\mathbf{k} = k_x\hat{x} + k_z\hat{z}$ the inertial Alfvén wave has the dispersion

$$\omega^2 = \frac{k_z^2 v_A^2}{1 + k_x^2 c^2/\omega_{pe}^2}, \tag{4}$$

and associated group velocity given by

$$\omega \frac{\partial \omega}{\partial \mathbf{k}} = \frac{k_z v_A^2}{1 + k_x^2 c^2/\omega_{pe}^2}\hat{z} - \frac{k_z^2 v_A^2 k_x c^2/\omega_{pe}^2}{[1 + k_x^2 c^2/\omega_{pe}^2]^2}\hat{x}. \tag{5}$$

Because of the minus sign in the x-direction term, the inertial wave is a backwards wave in the direction perpendicular to the equilibrium magnetic field.

B. Kinetic Alfvén waves

If $v_A < v_{Te}$ (which corresponds to $\beta_e > m_e/m_i$) then the electron parallel response becomes kinetic. Also, if the ion temperature is comparable to the electron temperature, then finite ion Larmor radius effects become important. Taking these into account gives the slab dispersion relation[11]

$$\omega^2 = k_z^2 v_A^2 \left(1 + k_x^2 \rho_i^2 \left(\frac{3}{4} + \frac{T_e}{T_i}\right)\right), \tag{6}$$

where the term involving 3/4 comes from finite ion Larmor radius (FLR) and the term involving T_e/T_i comes from parallel electron kinetics. Since the FLR and parallel electron kinetic terms have a qualitatively similar effect, for simplicity we will consider only electron kinetics, i.e., ignore the term involving 3/4. The group velocity for the kinetic Alfvén wave is given by

$$\omega \frac{\partial \omega}{\partial \mathbf{k}} = k_z v_A^2 (1 + k_x^2 \rho_s^2)\hat{z} + k_z^2 v_A^2 k_x \rho_s^2 \hat{x}, \tag{7}$$

where $\rho_s^2 = \kappa T_e/m_i\omega_{ci}^2$ can be considered as an effective ion gyro-radius. The kinetic wave is a forwards wave in the direction perpendicular to the equilibrium magnetic field.

V. MAGNETIC RECONNECTION AS A RADIATOR OF SHEAR ALFVÉN WAVES

The wave behavior of the inertial and kinetic regimes differ in many respects, but also have many similarities. Before analyzing these regimes individually, we will first examine what is common to both regimes, namely the following: localized magnetic reconnection is intimately related to the excitation of torsional Alfvén waves (also called shear Alfvén waves).

From a mathematical point of view, the magnetic field in the localized reconnection region can be described as $\mathbf{B}(\mathbf{x},t) = B_{z0}\hat{z} + \nabla A_z(\mathbf{x},t) \times \hat{z}$ where

$$A_z(\mathbf{x},t) = -B_{y0} a [\ln(\cosh(x/a)) + f(t) e^{-\rho^2/2a^2 - z^2/2h^2}]. \tag{8}$$

Here $f(t) = [1 + \tanh(t/\tau_{recon})]/2$ represents the ''switching on'' of reconnection in the characteristic time τ_{recon}, a is the characteristic width of the current filament in the reconnection layer, $\rho^2 = x^2 + y^2$, and $B_{y0} \ll B_{z0}$. The ''before'' sketch in Fig. 1(c) corresponds to level contours in the $z = 0$ plane of A_z for $t \ll -\tau_{recon}$ when $f(t) = 0$ so that $B_y(\mathbf{x},t) = B_{y0} \tanh(x/a)$; the ''after'' sketch corresponds to level contours of A_z for $t \gg \tau_{recon}$ when $f(t) = 1$. Since the current is $\mu_0 \mathbf{J} = \nabla \times (\nabla \times A_z\hat{z})$ the parallel component of the current is

$$J_z(t) = \frac{B_{y0}}{\mu_0 a}\left\{\frac{1}{\cosh^2(x/a)} - \left(2 - \frac{\rho^2}{a^2}\right) f(t) e^{-\rho^2/2a^2 - z^2/2h^2}\right\}. \tag{9}$$

Because Alfvén radiation has not been taken into account in Eqs. (8) and (9), these equations should be understood as near-field equations which apply only in the reconnection region $\rho \lesssim a$, $|z| \lesssim h$; this means that a must be smaller than the radial Alfvén wavelength and h must be smaller than the axial Alfvén wavelength. Equation (9) shows that reconnection effectively adds a filament of field-aligned bucking current of length h and radius a which reverses the initial field-aligned current that existed before the x-point developed. This reversal can be seen qualitatively by examining Fig. 1(c): the sense of the xy-plane magnetic field *in the reconnection region* is counterclockwise in the ''before'' sketch but is clockwise in the ''after'' sketch. It should be emphasized that the actual value of the reconnection time τ_{recon} is not predicted by our model; τ_{recon} is an input parameter and therefore the reconnection rate is guaranteed to be τ_{recon}^{-1}. However, whatever τ_{recon} happens to be in any actual reconnection situation, there must necessarily be a transient field-aligned current as given by the time-dependent part of Eq. (9).

We assume that the dynamics in the reconnection region are similar to conventional reconnection models and focus attention on finding an effective dissipation mechanism which allows the finite E_z to exist; in other words we are not proposing new dynamics in the reconnection region, but instead are proposing a new dissipation mechanism in the reconnection region. We divide the plasma into two regions: (i) a *control volume* of length h and radius a containing just the field-aligned transient current filament $I(t) \sim \pi a^2 J_z(t)$ described by Eq. (9), and (ii) the *external plasma* (everything outside the control volume). The external plasma responds to changes in the control volume, closes the current in the control volume so as to maintain $\nabla \cdot \mathbf{J} = 0$, and has propagating Alfvén waves described by the appropriate Maxwell–Lorentz equations. The $\tanh(t/\tau_{recon})$ time dependence in $I(t)$ can be thought of as a half-period of oscillation at a frequency

$$\omega \sim \pi/\tau_{recon}. \tag{10}$$

The transient control volume current thus acts as an antenna of length $\approx h$ which radiates Alfvén waves with frequency given by Eq. (10) into the plasma. The length h and oscillation frequency ω are constrained by the simultaneity condition, Eq. (3).

VI. PARALLEL DYNAMICS OF ALFVÉN WAVES

Using the linearized Vlasov equation to describe parallel dynamics, the parallel current may be expressed as

$$\mu_0\tilde{J}_z=\mu_0\sum_{\sigma=i,e}q_\sigma\int dv_z v_z\tilde{f}_\sigma$$

$$=\tilde{E}_z\sum_{\sigma=i,e}\frac{i\omega Z'(\zeta_\sigma)}{2k_z^2\lambda_{D\sigma}^2c^2}, \tag{11}$$

where Z is the plasma dispersion function, $\zeta_\sigma=\omega/k_z v_{T\sigma}$, and $v_{T\sigma}=\sqrt{2\kappa T_\sigma/m_\sigma}$.

Fluid dispersion relations show that ω/k_z is of the order of the Alfvén velocity v_A and also that the inertial Alfvén wave dispersion relation is obtained for $\omega/k_z\gg v_{Te}$ while the kinetic Alfvén dispersion relation is obtained in the opposite limit. Since $v_A=v_{Te}$ corresponds to $\beta_e=m_e/m_i$, it is seen that the inertial Alfvén regime occurs for $\beta_e<m_e/m_i$ while the kinetic regime occurs for $\beta_e>m_e/m_i$.

Inertial Alfvén waves: Here $\omega/k_z\gg v_{Te}$ and so we use

$$\lim_{\zeta\gg1}Z'(\zeta)=\zeta^{-2}-2i\pi^{1/2}\zeta\,\exp(-\zeta^2),$$

so that Eq. (11) becomes

$$\mu_0\tilde{J}_z=\tilde{E}_z\frac{i\omega_{pe}^2}{\omega c^2}\left[1-2i\pi^{1/2}\left(\frac{\omega}{k_z v_{Te}}\right)^3\exp(-\omega^2/k_z^2v_{Te}^2)\right]. \tag{12}$$

This shows that inertial Alfvén waves Landau damp on electrons as ω/k_z becomes of the order of v_{Te}. Hence, in a collisionless plasma, inertial Alfvén waves should heat electrons.

Kinetic Alfvén waves: Here $v_{Ti}\ll\omega/k_z\ll v_{Te}$ and so we use

$$\lim_{\zeta\ll1}Z'(\zeta)=-2-2i\pi^{1/2}\zeta\,\exp(-\zeta^2),$$

so that Eq. (11) becomes

$$\mu_0\tilde{J}_z=-\frac{i\omega\tilde{E}_z}{k_z^2\lambda_{De}^2c^2}\left[1+i\pi^{1/2}\sqrt{\frac{T_i}{T_e}}\frac{\omega}{k_z v_{T_i}}\left\{\sqrt{\frac{m_e}{m_i}}+\left(\frac{T_e}{T_i}\right)^{3/2}\exp(-\omega^2/k_z^2v_{T_i}^2)\right\}\right]. \tag{13}$$

The parallel dynamics are similar to that of ion acoustic waves and, in particular, it is seen that ion Landau damping (the last term in the above equation) dominates. Thus, kinetic Alfvén waves should heat ions. Furthermore, the resonant interaction is with ions having velocities $v\sim v_A$ so that wave energy will go into forming an ion tail with velocity of order v_A. This corresponds to a very energetic ion tail, since if the bulk ion thermal velocity were of order the Alfvén velocity, then the bulk ion β would be unity. One therefore expects Landau damping of kinetic Alfvén waves to result in suprathermal ions if $m_e/m_i\ll\beta_e\ll1$.

VII. EVALUATION OF THE RADIATION RESISTANCE

The radiation resistance is calculated by adapting to the Alfvén frequency regime a method[12,13] previously used for high frequency electron plasma waves. The control volume current is related to the fields and currents in the external plasma via Faraday's and Ampere's laws,

$$\nabla\times\tilde{\mathbf{E}}=i\omega\tilde{\mathbf{B}}, \tag{14}$$

$$\nabla\times\tilde{\mathbf{B}}=\mu_0(\tilde{\mathbf{J}}^{pl}+\tilde{\mathbf{J}}^{ant}), \tag{15}$$

where $\tilde{\mathbf{J}}^{pl}$ are the currents in the external plasma and $\tilde{\mathbf{J}}^{ant}$ is the current in the control volume. Note that $\nabla\cdot(\tilde{\mathbf{J}}^{pl}+\tilde{\mathbf{J}}^{ant})=0$ so that charge neutrality is always satisfied and currents may flow between the control volume and the external plasma. For an observer located in the plasma at some distance from the control volume, the control volume appears as a field-aligned radio antenna with current density

$$\tilde{\mathbf{J}}^{ant}=(2\pi\rho)^{-1}\delta(\rho)I(z)\hat{z}, \tag{16}$$

where $I(z)$ gives the axial distribution of current in the control volume. The plasma currents are determined by the Lorentz equation and since $B_y\ll B_{z0}$ the equilibrium magnetic field in the external plasma can be considered uniform and in the z-direction. The parallel current in the plasma region is given by either Eq. (12) or (13) depending on whether v_{Te} is large or small compared to v_A. In both cases the perpendicular plasma current is $\mu_0\tilde{J}_\rho^{pl}=-i\omega\tilde{E}_\rho/v_A^2$; this current corresponds to ion polarization current and is the same as the perpendicular current predicted by ideal MHD. From symmetry, $\tilde{J}_\theta^{pl}=0$.

We Fourier analyze in z, so all quantities are of the form $f(\rho,z)=(2\pi)^{-1}\int f(\rho,k_z)e^{ik_zz}dk_z$. By eliminating $\tilde{\mathbf{B}}$ between Eqs. (14) and (15) a vector wave equation is obtained. For kinetic Alfvén waves the z-component of this wave equation is

$$\frac{ik_z}{\rho}\frac{\partial}{\partial\rho}(\rho\tilde{E}_\rho)-\frac{1}{\rho}\frac{\partial}{\partial\rho}\left(\rho\frac{\partial}{\partial\rho}\tilde{E}_z\right)-\frac{\omega^2}{k_z^2\lambda_{De}^2c^2}\tilde{E}_z=i\omega\mu_0\tilde{J}^{ant}, \tag{17}$$

while for inertial waves the z-component is

$$\frac{ik_z}{\rho}\frac{\partial}{\partial\rho}(\rho\tilde{E}_\rho)-\frac{1}{\rho}\frac{\partial}{\partial\rho}\left(\rho\frac{\partial}{\partial\rho}\tilde{E}_z\right)+\frac{\omega_{pe}^2}{c^2}\tilde{E}_z=i\omega\mu_0\tilde{J}^{ant}. \tag{18}$$

For both inertial and kinetic waves the ρ-component is

$$\tilde{E}_\rho=\frac{ik_z}{\omega^2/v_A^2-k_z^2}\frac{\partial\tilde{E}_z}{\partial\rho}. \tag{19}$$

Substituting for $\tilde{E}_\rho$ in either Eqs. (17) or (18) gives the scalar wave equation

$$\frac{1}{\rho}\frac{\partial}{\partial\rho}\left(\rho\frac{\partial\tilde{E}_z}{\partial\rho}\right)+\kappa^2\tilde{E}_z=i\omega\varepsilon_A\mu_0\tilde{J}^{ant}, \tag{20}$$

where

$$\varepsilon_A = k_z^2 v_A^2/\omega^2 - 1 \tag{21}$$

and

$$\kappa^2 = \begin{cases} -\varepsilon_A \omega^2/c^2 k_z^2 \lambda_{De}^2, & \text{for kinetic waves,} \\ +\omega_p^2 \varepsilon_A/c^2, & \text{for inertial waves.} \end{cases} \tag{22}$$

For simplicity, we have omitted the Landau damping terms here, but it should be understood that these terms do exist and will ultimately attenuate the wave with a resulting transfer of energy to particles (electrons for an inertial wave, ions for a kinetic wave).

In the large ρ limit and setting $\kappa = k_\perp$, Eq. (22) becomes the kinetic or inertial Alfvén wave dispersion relations, Eqs. (4) and (6). From these dispersion relations it is seen that for inertial Alfvén waves ε_A is positive while for kinetic Alfvén waves ε_A is negative; i.e., the parallel phase velocity is slower than v_A for inertial waves, and faster than v_A for kinetic waves. From Faraday's law, the magnetic field is

$$\tilde{B}_\theta = \frac{1}{i\omega\varepsilon_A}\frac{\partial \tilde{E}_z}{\partial \rho}. \tag{23}$$

The homogenous radiative solutions of Eq. (20) are linear combinations of the Hankel functions $H_0^{(1)}(\kappa\rho)$, $H_0^{(2)}(\kappa\rho)$.

Substituting the explicit antenna current in Eq. (20), multiplying by ρ and integrating from 0 to ρ, gives the jump condition in the vicinity of $\rho = 0$,

$$\lim_{\rho \to 0} \rho \frac{\partial \tilde{E}_z}{\partial \rho} = \frac{i\omega\varepsilon_A \mu_0 \tilde{I}(k_z)}{2\pi}. \tag{24}$$

The causality condition of outward power flow from the antenna means that only solutions having radially outward group velocities are allowed. Since the inertial wave is a backwards wave in the radial direction, only the $H_0^{(2)}$ function is allowed for inertial waves, whereas since the kinetic wave is a forwards wave in the radial direction only the $H_0^{(1)}$ function is allowed for kinetic waves.

Thus, using $\lim_{s\to 0} dH_0^{(1)}(s)/ds = +2i/\pi s$ and $\lim_{s\to 0} dH_0^{(2)}(s)/ds = -2i/\pi s$ the desired solutions for the inhomogeneous wave equations are found to be

$$\tilde{E}_z(k_z) = \begin{cases} +\frac{1}{4}\omega\varepsilon_A\mu_0\tilde{I}(k_z)H_0^{(1)}(\kappa\rho), & \text{for kinetic waves,} \\ -\frac{1}{4}\omega\varepsilon_A\mu_0\tilde{I}(k_z)H_0^{(2)}(\kappa\rho), & \text{for inertial waves,} \end{cases} \tag{25}$$

with

$$\tilde{B}_\theta(k_z) = \begin{cases} -\frac{1}{4}i\mu_0\tilde{I}(k_z)\partial H_0^{(1)}(\kappa\rho)/\partial\rho, & \text{for kinetic waves,} \\ \frac{1}{4}i\mu_0\tilde{I}(k_z)\partial H_0^{(2)}(\kappa\rho)/\partial\rho, & \text{for inertial waves.} \end{cases} \tag{26}$$

We now calculate the radiated power from the antenna using the average power flux determined by the Poynting vector $\mathbf{S} = (2\mu_0)^{-1}\,\mathrm{Re}(\tilde{\mathbf{E}}\times\tilde{\mathbf{B}}^*)$. The time averaging of the Poynting vector is such as to eliminate second harmonics and so can be done over the time interval π/ω. The radial component of the Poynting vector is $S_\rho = -(2\mu_0)^{-1}\,\mathrm{Re}(\tilde{E}_z\tilde{B}_\theta^*)$ and the total emitted power will be the Poynting flux through a cylindrical surface infinitely long in the z direction and of radius ρ. This total radiated power will therefore be

$$P_{rad} = -\mu_0^{-1}\pi\rho\ \mathrm{Re}\int_{-\infty}^{\infty} dz \tilde{E}_z(z)\tilde{B}_\theta^*(z), \tag{27}$$

or using Parseval's theorem,

$$P_{rad} = -(2\mu_0)^{-1}\rho\ \mathrm{Re}\int_{-\infty}^{\infty} \tilde{E}_z(k_z)\tilde{B}_\theta^*(k_z)dk_z. \tag{28}$$

Substituting for $\tilde{E}_z(k_z)$ and $\tilde{B}_\theta^*(k_z)$ gives

$$P_{rad} = \frac{\omega\mu_0\rho}{32}\mathrm{Im}\int_{-\infty}^{\infty} \varepsilon_A|\tilde{I}(k_z)|^2 H_0^{(j)}(\kappa\rho) \times \frac{\partial H_0^{*(j)}(\kappa\rho)}{\partial\rho}dk_z, \tag{29}$$

where $j=1$ for kinetic waves and $j=2$ for inertial waves. At this point, the behaviors of kinetic and inertial waves differ sufficiently that it is best to consider these waves separately.

VIII. RADIATION RESISTANCE FOR KINETIC ALFVÉN WAVES

From Eq. (22) it is seen that for kinetic waves κ^2 is real only if $k_z^2 v_A^2/\omega^2 < 1$. If κ^2 is imaginary, then the Hankel functions become pure real, in which case the imaginary part of the integrand in Eq. (29) vanishes. Thus, radiated power occurs only when κ^2 is real, so that the range $|k_z| > \omega/v_A$ does not contribute to the integral and may be omitted.

Because the integrand in Eq. (29) is an even function of k_z and $[H_0^{(1)}(s)]^* = H_0^{(2)}(s)$, Eq. (29) can be written as

$$P_{rad} = \frac{\omega\mu_0\rho}{16}\mathrm{Im}\int_0^{\omega/v_A} \varepsilon_A|\tilde{I}(k_z)|^2 H_0^{(1)}(\kappa\rho) \times \frac{\partial H_0^{(2)}(\kappa\rho)}{\partial\rho}dk_z. \tag{30}$$

Using the Wronskian relation $H_0^{(2)}(s)\partial H_0^{(1)}(s)/\partial s - H_0^{(1)}(s) \times \partial H_0^{(2)}(s)/\partial s = 4i/\pi s$ it is readily seen that

$$\mathrm{Im}\, H_0^{(1)}(\kappa\rho)\partial H_0^{(2)}(\kappa\rho)/\partial\rho = -2/\pi\rho, \tag{31}$$

so that the radiated power for kinetic Alfvén waves becomes

$$P_{rad} = -(8\pi)^{-1}\omega\mu_0\int_0^{\omega/v_A}\varepsilon_A|\tilde{I}(k_z)|^2 dk_z. \tag{32}$$

Since the axial current profile is $\tilde{I}(z) = I_0\exp(-z^2/2h^2)$ its Fourier transform is $\tilde{I}(k_z) = I_0 h\sqrt{2\pi}\exp(-k_z^2h^2/2)$. Using this current spectrum and Eq. (21) gives

$$P_{rad} = \frac{\omega\mu_0}{4}I_0^2h^2\int_0^{\omega/v_A}\left(1 - \frac{k_z^2v_A^2}{\omega^2}\right)\exp(-k_z^2h^2)dk_z. \tag{33}$$

Since $h \ll \omega/v_A$ has been assumed, the argument of the exponential is always small giving the power radiated by the antenna to be

$$P_{rad} \simeq \frac{\omega^2\mu_0 I_0^2 h^2}{6v_A}. \tag{34}$$

TABLE I. Kinetic Alfvén wave radiation resistance for a selection of plasmas having $\beta_e > m_e/m_i$.

Kinetic Alfvén Wave	n	T_e	B	a	c/ω_{pe}	τ_{ei}	τ_{recon}	h	$\frac{\eta_{rad}}{\eta_{Spitz}}$	$\frac{\eta_{rad}}{\eta_{inertia}}$
	m^{-3}	eV	T	m	m	s	s	m		
MRX (Ref. 14)	10^{20}	20	3×10^{-2}	1.5×10^{-2}	5×10^{-4}	3×10^{-8}	10^{-5}	0.1	2	10^3
Large tokamak (core)	10^{20}	10^4	5	2×10^{-3}	5×10^{-4}	2×10^{-4}	10^{-4}	2×10^2	2×10^1	2×10^1
PSBL, slow	10^5	150	2×10^{-8}	6×10^4	1.6×10^4	2×10^8	10^2	2×10^7	2×10^7	2×10^1
PSBL, fast	"	"	"	"	"	2×10^8	1	2×10^5	2×10^9	2×10^1
Lobe (warm, slow)	10^4	10^2	2×10^{-8}	5×10^4	5×10^4	10^9	100	7×10^7	10^7	2
Lobe (warm, fast)	10^4	10^2	2×10^{-8}	5×10^4	5×10^4	10^9	1	7×10^5	10^9	2
Solar corona	10^{15}	200	10^{-2}	0.1	0.2	5×10^{-2}	10^2	10^8	3×10^{-4}	1

Using $P_{rad}=I_0^2R$ the antenna radiation resistance is

$$R=\frac{\omega^2h^2}{6v_Ac}\sqrt{\frac{\mu_0}{\varepsilon_0}}. \tag{35}$$

Assuming the antenna radius (thickness of reconnection layer current filament) to be a, the effective resistivity due to Alfvén wave radiation will be $\eta_{rad}=\pi a^2R/h$ or

$$\eta_{rad}=\frac{\pi\mu_0\omega^2a^2h}{6v_A}. \tag{36}$$

If we define

$$\alpha=\omega h/v_A, \tag{37}$$

then from Eq. (3) α must always be smaller than unity. Using Eq. (37) to eliminate h and using Eq. (10) for ω, the kinetic Alfvén wave radiation resistivity becomes

$$\eta_{rad}=\frac{\pi^2\mu_0\alpha a^2}{6\tau_{recon}}. \tag{38}$$

This is an important result because it shows that radiation resistivity gives an effective diffusion coefficient $D_{rad}=\eta_{rad}/\mu_0$ which is consistent with the observed magnetic diffusion rate $\sim a^2/\tau_{recon}$.

The ratio of kinetic Alfvén wave radiation resistivity to Spitzer resistivity, Eq. (1), is

$$\frac{\eta_{rad}}{\eta_{Spitz}}=\frac{\pi^2\alpha}{6}\left(\frac{a}{c/\omega_{pe}}\right)^2\frac{\tau_{ei}}{\tau_{recon}}. \tag{39}$$

Using $\tau_{recon}\sim\tau_{acc}$, the ratio of kinetic Alfvén wave resistivity to the inertial resistivity given by Eq. (2) is

$$\frac{\eta_{rad}}{\eta_{inertia}}=\frac{\pi^2\alpha}{3}\left(\frac{a}{c/\omega_{pe}}\right)^2. \tag{40}$$

Table I lists characteristic parameters for a variety of plasma regimes and gives η_{rad}/η_{Spitz} calculated using Eq. (39) and the assumption $\alpha=1/2$.

We assumed in Eq. (16) that the antenna appears to an observer in the far field to behave as a delta-function in the radial direction. Delta-function behavior in the radial direction means that the antenna radius is small compared to the natural radial scale length of the partial differential equation. Since this natural radial scale length is the wave radial wavelength, the antenna radius must not exceed the characteristic radial wavelength of the wave. Equivalently, the antenna radius must be sufficiently small that the antenna radius is in the near-field region [see the discussion after Eq. (9)] so that retarded time effects across the antenna radius are negligible. Since the perpendicular wavelength is of the order ρ_s for the kinetic wave, we conclude that the antenna radius cannot exceed ρ_s in order for the antenna to be characterized by Eq. (16). Recent experiments on the Magnetic Reconnection Experiment (MRX)[14] indicate that the thickness of the reconnection layer in the kinetic regime is of the order of ρ_s. Thus, the antenna radius is bounded from both above and from below by ρ_s and so it is reasonable to assume that the antenna current filament radius is $a\sim\rho_s=(\kappa T_e/m_i)^{1/2}/\omega_{ci}$. The characteristic reconnection time τ_{recon} is an estimate based on observations.

Table I shows that radiation resistance is larger than the Spitzer resistivity for all the plasmas listed with the exception of the solar corona which is quite collisional. The values of h are reasonable for MRX[14] and the magnetotail plasmas [plasma sheet boundary layer (PSBL), warm tail lobe], but for the large tokamak the radiating current channel would have to go around the torus many times (which might be possible). The length h for the solar plasma is comparable to the size of solar structures and is probably too large to be considered as an antenna radiating to infinity. It is reasonable to conclude that radiation resistance is consistent with observed reconnection times in the magnetotail provided the current channel width is indeed a, and the axial length of the reconnection region is indeed h. Radiation resistance is also likely important in the MRX experiment and the core of hot tokamaks. For the solar plasma, the current sheet width of 0.1 m is very small compared to the overall dimensions so that it is probably unrealistic to characterize reconnection in this case as the time for a magnetic field to diffuse the distance a.

IX. INERTIAL ALFVÉN WAVE RADIATION RESISTANCE

From Eq. (22) it is seen that for inertial waves κ^2 is real only if $k_z^2v_A^2/\omega^2>1$. Since radiated power occurs only when κ^2 is real, the range $-\omega/v_A<k_z<\omega/v_A$ does not contribute to the integral and may be omitted. Thus, in this case Eq. (29) becomes

TABLE II. Inertial Alfvén wave radiation resistance for a selection of plasmas having $\beta_e < m_e/m_i$.

Inertial Alfvén Wave	n	T_e	B	amu	$\beta m_i/m_e$	c/ω_{pe}	τ_{recon}	h	$\frac{\eta_{rad}}{\eta_{Spitz}}$	$\frac{\eta_{rad}}{\eta_{inertia}}$
	m^{-3}	eV	T			m	s	m		
Large tokamak (edge)	10^{19}	10^3	5	2	0.6	1.6×10^{-3}	10^{-4}	4×10^2	0.7	0.6
Magnetotail lobe (cold)	10^4	10	2×10^{-8}	1	0.2	5×10^4	100	7×10^7	4×10^6	3
Near-earth magnetosphere	10^{10}	1	3×10^{-5}	16	0.1	5×10^1	1	3×10^5	2×10^1	6

$$P_{rad}=\frac{\omega\mu_0\rho}{16}\,\mathrm{Im}\int_{\omega/v_A}^{\infty}\varepsilon_A|\tilde{I}(k_z)|^2H_0^{(2)}(\kappa\rho)\times\frac{\partial H_0^{(1)}(\kappa\rho)}{\partial\rho}dk_z. \tag{41}$$

Using the Wronskian relation as in the previous section, the radiated power becomes

$$P_{rad}=(8\pi)^{-1}\omega\mu_0\int_{\omega/v_A}^{\infty}\varepsilon_A|\tilde{I}(k_z)|^2dk_z. \tag{42}$$

Because $k_z<\omega/v_{Te}$ is assumed for the inertial wave, the upper limit of the k_z integration cannot be at infinity and instead must be truncated[13] at $k_z=\omega/v_{Te}$ so the radiated power becomes

$$P_{rad}=\frac{\omega\mu_0I_0^2h^2}{4}\int_{\omega/v_A}^{\omega/v_{Te}}\varepsilon_A\,\exp(-k_z^2h^2)dk_z. \tag{43}$$

Assuming again that the argument of the exponential is small in order to satisfy Eq. (3), the total radiated power will therefore be

$$P_{rad}=(4v_A)^{-1}\mu_0I_0^2h^2\omega^2\int_1^{\gamma_T}(\gamma^2-1)d\gamma, \tag{44}$$

where $\gamma_T=v_A/v_{Te}$. In the limit of a very cold plasma, i.e., $\gamma_T\gg1$, this becomes

$$P_{rad}\simeq\frac{I_0^2\omega^2h^2v_A^2}{12v_{Te}^3c}\sqrt{\frac{\mu_0}{\epsilon_0}}. \tag{45}$$

Using $P=I_0^2R$ the antenna radiation resistance is

$$R_{rad}=\frac{\omega^2h^2v_A^2}{12v_{Te}^3c}\sqrt{\frac{\mu_0}{\epsilon_0}}, \tag{46}$$

which reverts to Eq. (45) of Ref. 13 if v_A is replaced by c. The resistivity will be

$$\eta_{rad}=\frac{\omega^2hv_A^2\pi a^2\mu_0}{12v_{Te}^3}, \tag{47}$$

and using $h=\alpha v_A/\omega$, $\omega=\pi/\tau_{recon}$ this becomes

$$\eta_{rad}=\frac{\alpha\pi^2}{12}\frac{a^2\mu_0}{\tau_{recon}}\frac{v_A^3}{v_{Te}^3}. \tag{48}$$

If α is of order unity, this resistivity is a factor $(v_A/v_{Te})^3$ larger than what is required for diffusion of the magnetic field across the distance a in a time τ_{recon} which suggests that smaller α might occur.

We now compare the radiation resistance to the Spitzer and electron inertia resistivity. Because both η_{rad} and η_{Spitz} scale as $v_{Te}^{-3/2}$ it is worthwhile expressing the Spitzer resistivity in terms of fundamental quantities,

$$\eta_{Spitz}=\frac{1.7m_e^{1/2}Ze^2\ln\Lambda}{32\pi^{1/2}\varepsilon_0^2(2\kappa T_e)^{3/2}}. \tag{49}$$

From Eqs. (1) and (48) the ratio of inertial Alfvén wave resistivity to Spitzer resistivity is

$$\frac{\eta_{rad}}{\eta_{Spitz}}=\frac{15\alpha}{Z\ln\Lambda}\frac{nv_A^3a^2}{\omega_{pe}^2\tau_{recon}c^2}. \tag{50}$$

From Eqs. (2) and (48) the ratio of radiation resistance to inertial resistance is

$$\frac{\eta_{rad}}{\eta_{inertial}}=\frac{\pi\alpha}{6}\frac{v_A^3}{v_{Te}^3}\frac{\omega_{pe}^2a^2}{c^2}, \tag{51}$$

where we have used $\tau_{acc}\sim\tau_{recon}$ since for a cold plasma the electron acceleration time is the same as the time required to form the field-aligned current.

As noted in the paragraph after Eq. (40) the antenna radius must not exceed the Alfven wave radial wavelength. For the inertial wave this wavelength $\sim c/\omega_{pe}$ and so the antenna radius should not exceed $\sim c/\omega_{pe}$. If there were no radiation resistance and the plasma was collisionless, the thickness of the reconnection region would be[1,4,5,15] the electron skin depth, c/ω_{pe}. Thus, the reconnection region must be at least $a=c/\omega_{pe}$, the value predicted by inertial reconnection, but cannot be substantially larger because if it were, the antenna radius would exceed the characteristic radial wavelength of the wave and so not be in the near field. The antenna radius is thus bounded both from below and from above by $\sim c/\omega_{pe}$ and so we conclude that the effective antenna radius is $\sim c/\omega_{pe}$ in the inertial regime.

Using $a=c/\omega_{pe}$ gives $\eta_{rad}/\eta_{inertial}>\alpha v_A^3/v_{Te}^3=\alpha(m_i\beta_e/m_e)^{-3/2}$. Since $\beta_em_i/m_e<1$ for inertial waves, the effective resistivity due to radiation resistance will typically be larger than the inertial resistance. Thus, radiation resistance is clearly important when $\beta\ll m_e/m_i$. Examples of plasmas having $\beta<m_e/m_i$ are the edge of large tokamaks, the near-earth magnetosphere, and on occasion, the magnetotail lobes. Table II compares the radiation resistance for inertial Alfvén waves to the Spitzer and inertial resistivities for these regimes. The current filament radius is assumed to be of the order of the electron skin depth, c/ω_{pe}.

As before, the reconnection time is based on typical observations while h is calculated assuming $\alpha = 1/2$.

From Table II it is seen that radiation resistance should be dominant in the near-earth magnetosphere and also in the magnetotail lobe when cold. In the edge of a large tokamak, Spitzer resistivity, inertial resistivity, and radiation resistivity are all comparable suggesting that significant inertial Alfvén wave radiation should be expected in conjunction with reconnection.

X. SUMMARY AND CONCLUSION

By comparing the magnetic field topologies before and after reconnection, it is seen that reconnection necessarily involves a transient field-aligned current filament. In the kinetic regime the current filament radius is expected to be of the order of the ion gyroradius while in the inertial regime the current filament radius is expected to be of the order of the electron skin depth. The radiation resistance can be comparable to or larger than the inertial resistance for both kinetic and inertial regimes; for very collisionless plasmas, the radiation resistance is many orders of magnitude larger than the Spitzer resistance. If magnetic reconnection is considered as being mediated by an effective magnetic diffusion $a^2 \sim \eta\tau/\mu_0$, where η is an effective resistivity, then radiation resistance is sufficient to support this diffusion in many situations.

Radiation resistance is inherently missing from 2D models of reconnection, because 2D models effectively assume the axial coordinate is ignorable or periodic, and so ignore time retardation effects in the axial direction. In contrast, the analysis presented here takes into account time retardation which has the effect of introducing an in-phase component of E_z with J_z.

Our analysis is an order of magnitude estimate of the importance of radiation resistance and does not pretend to be a complete self-consistent solution of the reconnection-radiation dynamics. A complete self-consistent analysis would require the solution of systems of time-dependent partial differential equations having sufficient spatial resolution to describe both the fine-scale spatial–temporal structure of the reconnection process and the large-scale structure of the radiating Alfvén waves.

Landau damping will be important when collisionality is small, i.e., the regime when Spitzer resistivity is unimportant. Thus, in situations where radiation resistance is dominant (or even significant) energetic particles should be generated as a result of reconnection. This analysis thus provides a plausible explanation for the energetic particles so often seen to be associated with reconnection. The energetic particles are not created at the site of the reconnection, but are created instead at a distant location where the radiated wave undergoes Landau damping. In the $\beta_e \ll m_e/m_i$ regime the energetic particles will be parallel streaming electrons, while for the regime $m_e/m_i \ll \beta_e \ll 1$ the energetic particles will be parallel streaming ions. Finite ion Larmor radius (which has not been considered here) would likely result in perpendicular ion heating as well.

ACKNOWLEDGMENTS

Discussions with D. Rutledge regarding return currents in free-space (vacuum) antennas are gratefully acknowledged.

This work has been supported by the National Science Foundation.

[1] J. A. Wesson, Nucl. Fusion **30**, 2545 (1990).
[2] J. F. Drake, R. G. Kleva, and M. E. Mandt, Phys. Rev. Lett. **73**, 1251 (1994).
[3] Z. W. Ma and A. Bhattacharjee, Geophys. Res. Lett. **23**, 1673 (1996).
[4] M. Tanaka, Phys. Plasmas **2**, 2920 (1995).
[5] M. Tanaka, Comput. Phys. Commun. **87**, 117 (1995).
[6] S. Ramo and J. H. Whinnery, *Fields in Modern Radio*, 2nd ed. (Wiley, New York, 1953), pp. 222–225.
[7] H. Pfister and W. Gekelman, Am. J. Phys. **59**, 497 (1991).
[8] E. N. Parker, Astrophys. J. **174**, 499 (1972).
[9] S. J. Vainshtein and E. N. Parker, Astrophys. J. **304**, 821 (1986).
[10] W. Gekelman and H. Pfister, Phys. Fluids **31**, 2017 (1988).
[11] A. Hasegawa and C. Uberoi, ''The Alfvén wave'', United States Department of Energy Technical Information Center, DOE/TIC-11191, 1982, available from the National Technical Information Service, U.S. Dept. of Commerce, Springfield, Virginia, 22161.
[12] S. R. Seshradi, IEEE Trans. Antennas Propag. **AP-13**, 819 (1965).
[13] N. Singh and R. W. Gould, Radio Sci. **12**, 1151 (1971).
[14] M. Yamada, H. T. Ji, and S. Hsu, Phys. Plasmas **4**, 1936 (1997).
[15] C. E. Seyler, J. Geophys. Res. **95**, 17 199 (1990).